Color-to-Depth Mappings as Depth Cues in Virtual Reality

Zhipeng Li
lzp20@mails.tsinghua.edu.cn
Tsinghua University
Beijing, China

Yikai Cui
cbst987@live.cn
Tsinghua University
Beijing, China

Tianze Zhou
zhoutz19@mails.tsinghua.edu.cn
Tsinghua University
Beijing, China

Yu Jiang*
jiangyu0927@gmail.com
Tsinghua University
Beijing, China

Yuntao Wang
yuntaowang@tsinghua.edu.cn
Tsinghua University
Beijing, China

Yukang Yan†
yukangy@andrew.cmu.edu
Carnegie Mellon University
Pittsburgh, United States of America
Tsinghua University
Beijing, China

Michael Nebeling
nebeling@umich.edu
University of Michigan
Ann Arbor, United States of America

Yuanchun Shi
shiyc@tsinghua.edu.cn
Tsinghua University
Beijing, China

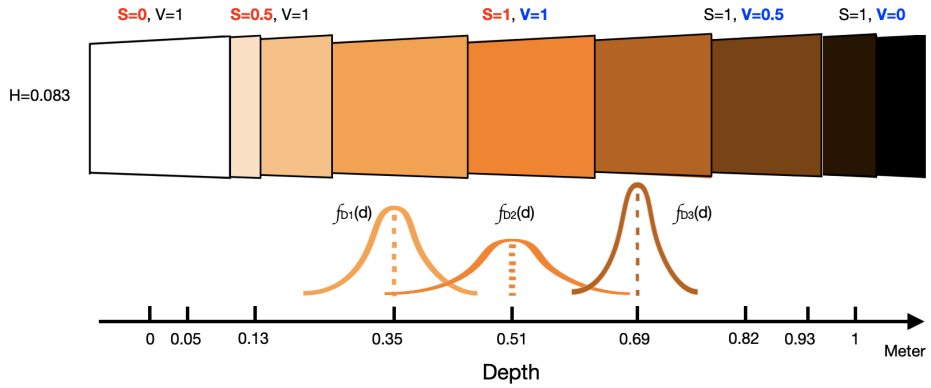

Figure 1: Color-to-depth mappings alter virtual objects' colors (H: Hue, S: Saturation, V: Value) to reflect their depths. We calculates intuitive mappings by inferring the confusion probability based on mapping data collected from users. Users map single color to a distribution of depths as illustrated by the curves, and the area under the intersected curves indicates the probability that they may map two colors to the same depth.

ABSTRACT

Despite significant improvements to Virtual Reality (VR) technologies, most VR displays are fixed focus and depth perception is still a key issue that limits the user experience and the interaction performance. To supplement humans' inherent depth cues (e.g., retinal blur, motion parallax), we investigate users' perceptual mappings of distance to virtual objects' appearance to generate visual cues aimed to enhance depth perception. As a first step, we explore color-to-depth mappings for virtual objects so that their appearance differs in saturation and value to reflect their distance. Through a series of controlled experiments, we elicit and analyze users' strategies of mapping a virtual object's hue, saturation, value and a combination of saturation and value to its depth. Based on the collected data, we implement a computational model that generates color-to-depth mappings fulfilling adjustable requirements on confusion probability, number of depth levels, and consistent saturation/value changing tendency. We demonstrate the effectiveness of color-to-depth mappings in a 3D sketching task, showing that compared to single-colored targets and strokes, with our mappings, the users were more confident in the accuracy without extra cognitive load

*This work was done while Yu Jiang was an intern at Tsinghua University.
†Denotes as the corresponding author.

UIST '22, October 29-November 2, 2022, Bend, OR, USA

ACM ISBN 978-1-4503-9320-1/22/10…$15.00
https://doi.org/10.1145/3526113.3545646

and reduced the perceived depth error by 60.8%. We also implement four VR applications and demonstrate how our color cues can benefit the user experience and interaction performance in VR.

CCS CONCEPTS

• **Human-centered computing → User models**.

KEYWORDS

Virtual reality, depth perception, color-to-depth mapping

ACM Reference Format:
Zhipeng Li, Yikai Cui, Tianze Zhou, Yu Jiang, Yuntao Wang, Yukang Yan, Michael Nebeling, and Yuanchun Shi. 2022. Color-to-Depth Mappings as Depth Cues in Virtual Reality. In *The 35th Annual ACM Symposium on User Interface Software and Technology (UIST '22), October 29-November 2, 2022, Bend, OR, USA.* ACM, New York, NY, USA, 14 pages. https://doi.org/10.1145/3526113.3545646

1 INTRODUCTION

Currently, VR devices produce the sense of virtual objects' depths by providing pictorial (e.g., shading [78] and occlusion), oculomotor (defocus blurring [51]), and binocular cues (e.g., binocular disparity [60]) that humans inherently rely on to perceive depth in reality. Given that most current VR displays are fixed focus, however, inaccuracies in users' perceived depths of virtual objects are common and can negatively impact the user experience in interaction tasks, e.g., when locating targets, trying to sketch precisely, or arranging user interfaces). In addition to prior efforts adding visual cues such as light field rendering [36] and ocular motion parallax [34] via advanced rendering techniques, we explore dynamically recoloring virtual content based on the VR user's position in the scene and distance to virtual objects to stimulate depth perception.

Mapping rendering attributes of objects (e.g., color [79], contrast [57, 78], opacity [59], level of blurriness [45, 46]) to depth is already an established technique in computer graphics research. However, as there are few best practices and common design guidelines, typically these mappings are defined manually by experienced visual designers, which requires professional training and expertise in human-computer interaction and human factors. At the core of this research is an investigation into how to dynamically generate color-to-depth mappings that are intuitive to users based on a set of controlled experiments. Based on our experiments, we develop a computational model that automatically calculates mappings so that it becomes easier for VR application designers and developers to respond to varying application requirements and user needs in terms of the number of distinguishable depth levels. We demonstrate that our model effectively reduces the probability for users to be confused about the visual cues and enables more accurate in depth perception in VR scenes on current headsets.

This paper offers three main contributions.

- We investigate how users intuitively map color space to depth axis to quantify how hue, value, and saturation should be altered to reflect depth changes separately and jointly.
- We construct a computational model to generate color-to-depth mappings that fulfill requirements for the number of depth levels and probability of color confusions.
- We evaluate the use and usability of the generated color-to-depth mappings in a comparative study in a VR sketching task, and demonstrate the benefits in four applications.

First, using the HSV color model instead of RGB since it is often regarded a more intuitive way to describe color the way users perceive it, we conducted a series of controlled experiments to understand how users map hue, saturation, and value channels separately, and colors in the combined space to depth in VR scenes. Results showed that hue-to-depth mappings were inconsistent across participants, while saturation-to-depth and value-to-depth mappings were linear in the whole range or part of the range; when mapping saturation-value space to the depth axis, participants' data points formed an approximate linear plane and provided more distinguishable depth levels than either single channel. As the second contribution, we developed a computational model that automatically generates color-to-depth mappings. We firstly built a statistical model based on data from user studies to measure the confusion probability that the user may misrecognize a color cue to another, and thus misperceive the depth that it represents. Based on the model, we developed an algorithm to search for a color-to-depth mapping that maximizes the number of depth levels while maintaining the confusion probability of every neighboring color cues under required limits. Among the candidates, the algorithm selects the mapping with the least average confusion probability. Using the algorithm, we built a color-to-depth mapping with eight distinguishable depth levels and evaluated it in a sketching task in comparison to a single-colored baseline method. Results showed that the generated mapping significantly increased the sketching accuracy by reducing the shape error by 72.98% and the depth error by 60.8% in 3D tasks. Further, participants were more confident in control accuracy without extra cognitive load. Finally, we implemented four VR applications, some of which were recreated from prior work, to demonstrate the potential benefits of the color-to-depth mappings generated by our model, and discuss extensions to other rendering attributes in future work.

2 RELATED WORK

2.1 Depth perception in VR

Inaccurate perception of depth in VR has been a long-standing problem [4, 29, 51, 58, 82] as studies have shown that users tend to underestimate the distance of further objects and overestimate the distance of closer objects [32, 53]. Extensive efforts have been devoted to identify factors causing depth misperception in VR [21, 25, 27, 35, 43, 73, 76]. Willemsen et al. [81] and Thompson et al. [71] investigated how low-quality computer-generated images lead to depth misperception. Willemsen et al. [80] revealed that the display's mechanical features (e.g., display weight) could also contribute to distance underestimation.

Despite the limited hardware, one main cause of depth perception is the lack of depth cues in VR. Loomis et al. [33, 42] and Sina Masnadi et al. [44] found that the narrow field of view could significantly influence the perceived depth in VR. Past research attempted to build on users' inherent depth cues, such as oculomotor (defocus blurring) [51], monocular [17, 26], and binocular depth cues [62], to alleviate depth misperception. Thomas et al. [70] leveraged the skybox and floor grids to provide monocular depth cues.

Vinnikov et al. [74] and Mauderer et al. [48] tracked the user's gaze during interaction to provide the oculomotor depth cue with the gaze-contingent depth of field. Though these research attempted to restore users' inherent depth cues in VR, the depth misperception still exists [31].

As a result, depth misperception has a profound influence on interactions in VR [38, 41]. The visual and vestibular system discrepancies induce motion sickness and dizziness [12, 28]. Cheng et al. [15] found that the hand-eye coordination ability in VR was influenced by depth perception. Nguyen et al. showed that users would have a depth perception conflict when the stereoscopic video and virtual UI elements were rendered simultaneously [55]. Arora et al. [5] pointed out that the depth misperception in VR limited users' performance in 3D sketching.

As a supplement to providing inherent depth cues, a different strategy is adding extra visual cues to the object's appearance to hint at its depth. It has been a common practice to add visual cues, including color [79], contrast [78], level of blurriness [45, 46] and other attributes to create a sense of depth in paintings, photographs, depth images, and virtual scenes. For instance, artists painted the further objects by decreasing their contrast and saturation to make them near to the background to simulate the atmosphere [1]. Distance fog [78] added fog in certain depth range to help users recognize the depth differences between objects in the front of, within, and behind the fog. Rößing et al. [65] provided the depth of field, contrast, occlusion and saturation as depth cues in 2D videos. However, we argue that there lacks a thorough investigation on users' perceptual mappings of distance to virtual objects' appearance. Such investigations are crucial in generating appropriate mappings between visual cues and depth in a computational manner. So in this paper, we take color (hue, saturation, value) as an example to elicit intuitive color-to-depth mappings from users and finally verify the benefits via evaluations and applications.

2.2 Color perception in interaction

Human beings perceive colors by using our visual system to interpret light stimulation coming from objects with various colors [47]. Though the stimulation could be changed by the strength and direction of the environment's light, users can identify colors consistently based on their knowledge of color perception [20]. This knowledge has been commonly leveraged to visualize scientific data [56, 68, 69, 86], present affective information [8, 10, 50], facilitate object recognition [14], etc. Löffler et al. leveraged color to increase the efficiency, effectiveness, and user satisfaction of interaction with tangible user interfaces [40]. Bartram et al. investigated how different color properties (lightness, chroma, and hue) presented affective information in visualizations [8]. As for using color to represent quantitative information, depth has also been represented using colormaps for decades [9, 61]. Artists have been using lighter colors to create a sense of depth for distant objects in 2D paintings [1]. Troscianko et al. [72] used color to encode depth in the real world while Bailey et al. [6, 7] and Weiskopf and Ertl [77] leveraged color's saturation and intensity to hint at virtual objects' depth with designer-chosen parameters. While in the depth images captured by RGBD cameras, depth is mapped to various colors to present the scene's morphology feature and depth at the same time [79]. Moreover, Angelopoulos et al. used colors to reflect specific ranges of depth for patients with Retinitis Pigmentosa in Augmented Reality [3]. Colormaps, as the encoding of color to visualized attributes mapping, is the key design that influences the perceptual efficiency in these applications [63]. The rainbow colormap, which includes the most saturated colors, has been the most frequently used colormap in visualization practice for years [39]. However, researchers have reported that the rainbow colormap could hinder information presentation due to its lack of perceptual ordering [13, 37, 64, 75]. Turbo [1] addressed the Jet's shortcomings with a hand-crafted and fine-tuned colormap and DepthLab [19] leveraged Turbo to integrate depth into mobile AR applications. Different from existing techniques that mapped colors to certain visual attributes, we propose to investigate how users perceptually map the 3D color space (hue, saturation, value) to the depth axis and generate efficient and intuitive color-to-depth mappings in a computational manner.

3 MAPPING COLOR SPACE TO DEPTH AXIS

As color can be characterized as a three-dimensional space (hue, saturation, value) while depth is a one-dimensional axes, it is unclear how to build mappings between them so that users can easily infer depth information with color cues. We decided to first disentangle the color dimensions by investigating how users map hue, saturation, and value separately to depth. Based on the results, we further investigated mappings between the (saturation, value) combination and depth. As multiple models are valid in representing the color space, we used the HSV color model, a commonly used model in literature, which describes a color with hue(**H**), saturation(**S**), and value(**V**) [8, 30, 52]. In this model, **H** decides the type of the color while **S** decides the whiteness of the color, and **V** determines the darkness of the color.

3.1 Phase 1: Mapping H to Depth

We first investigated how users map the hue spectrum to different depth levels.

3.1.1 Task. First of all, the task is not to ask participants to distinguish different colors (hues in this phase), it is to form a one-to-one mapping where participants will assign a depth value to the target hue. To achieve this goal, we referred to existing studies on depth estimation in VR to design the task. Yet we found other than evaluating how participants estimated depths, previous studies also required accurate movement control - users are often required to locate objects at target depth, for example walk themselves to the depth [41], or throw a ball to the target location [66]. In this regard, we refined the design to minimize the control bias while maintaining a good sense of depth. As shown in Figure 2, we rendered a trial square with a given color. We also put two referenced squares which formed a line with the trial square, one was at the front, and one was at the back, to rule the trial square's moving range. Participants were asked to move the trial square along the one-dimensional axis with the controller joystick and stop at a depth where they found the target color reflected most intuitively. This reduces the control requirement compared to walking or throwing balls. Meanwhile,

[1] https://ai.googleblog.com/2019/08/turbo-improved-rainbow-colormap-for.html

seeing the trial square's depth with respect to the reference squares maintained the sense of depth.

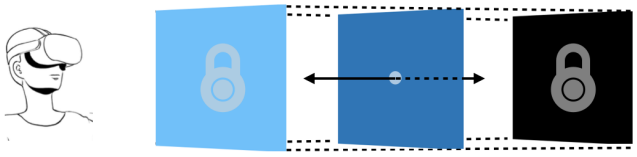

Figure 2: In the trials, we aligned two reference squares of the same color but with different hue, saturation, or value at opposite ends and inserted a trial square of the target color at a random position between the two reference points. The task was to move the trial square along the line between the reference squares such that the trial square's depth matches the color in the spectrum between the two reference squares.

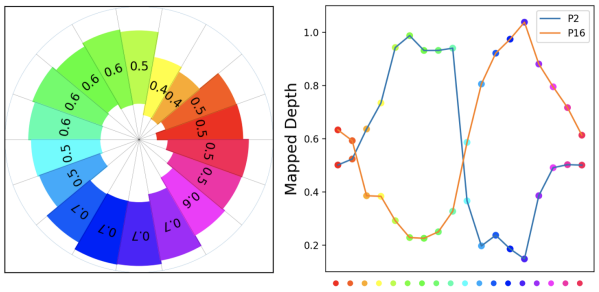

(a) (b)

Figure 3: (a) The mean and standard deviation of the mapped depth (meter) of each tested hue. The mean is texted over the wedge while also illustrated by its center's position. The wedge length indicated the standard deviation. (b) Two participants(P2, P16)' hue-to-depth mapping results.

3.1.2 Procedure. After ensuring the participants could observe the virtual environment clearly and comfortably, the researcher conducted a warm-up session to help them get familiar with the task. At the beginning of each trial, the participant was shown two references at the fixed positions and the trial square of the target color at a random initial position. The participant used the VR controller's joystick to move the trial square to the goal depth and pressed a button to confirm.

3.1.3 Design. The independent variable is **H**, and **S** and **V** are set as the control factors. The dependent variable is the depth where participants placed the trial square. We tested 18 **H** levels evenly distributed from 0 to 1 and set **S** and **V** fixed as 1 (with highest saturation and value). The two reference squares were white to only provide the depth reference. The height of all squares was set to 10 cm under the user's head. We showed all the tested colors to the user in the warm-up session. The 18 tested hues were repeated 5 times and appeared in a randomized order for each participant, resulting in $18 \times 5 = 90$ trials. The whole study lasted around 15 minutes. We studied the color-to-depth mapping in a hand-reachable depth range (10 cm to 110 cm in the front), which is one most frequently used space in VR applications. To control the influence of the virtual background, we conducted the study with a virtual white background.

3.1.4 Apparatus. We conducted the user study on the Oculus Quest 2 headset and implemented the experimental interface using Unity 2019. Participants sat comfortably on a chair during the experiment.

3.1.5 Participants. We recruited 16 participants (8 females and 8 males) from a local university. Participants were aged 19 to 32 with an average age of 23.38 (SD = 3.90). The average self-reported familiarity with VR score was 2.88 (SD = 1.26) with a 7-point Likert scale (1-not familiar at all, 4-neutral, 7-very familiar). All participants had normal vision and did not have color weakness or blindness.

3.1.6 Results. We calculated the average mapped depth and the standard deviation for each hue as shown in Figure 3a. The green-like (hue range 0.22 - 0.55) colors' mapped depths are 0.6 with a standard deviation of 0.26, which reflects that the participants tended to map them to a similar depth level. The mapped depth then increased to 0.7 on average when the color became the blue spectrum (hue range 0.55 - 0.88) and then reduced to 0.4 on average with the color changed to red and yellow (hue range 0.88 - 0.22). We conducted Repeated-Measures ANOVA ($p < 0.05$) with Bonferroni-corrected post-hoc T-test ($p < 0.05$) on the results to investigate if the **H** influenced the mean of mapped depth. Results showed that the **H** significantly affected the mapped depth ($F_{(17,255)} = 2.79$, $p < 0.001$) and post-hoc results revealed that only the mapped depth of yellow ($hue = 0.22$, $AVG = 0.37$, $SD = 0.18$) was significantly less than blue's ($hue = 0.72$, $AVG = 0.68$, $SD = 0.18$, $t = 4.46$, $p < 0.001$). Therefore, the mapped depth of each tested hue overlapped heavily with the neighboring hues, which suggests that there might not exist a consistent hue-to-depth mapping that most participants agree on. To further probe this phenomenon, we took a further look at individual mappings of participants. Figure 3b visualizes the two mappings created by P2 and P16, which appeared to be in an almost reverse pattern. We found similar results in the comparison between other participants. We reason that as hue appears to be a circled spectrum without a recognized starting hue, different participants may select their own starting hue with different rotating orders around the circle and some of them also created their own order. As a result, although hue has been widely used as the depth cue [1, 79], it is difficult for users to intuitively and consistently map it to the depth.

3.2 Phase 2: Mapping S and V to Depth separately

Different from the hue channel as a circled spectrum, saturation and value are ordinal channels that become stronger as the channel value increases. So we applied the same task to elicit the participants' mappings between **S**, **V** and depth separately in this phase.

3.2.1 Procedure and apparatus. The procedure and apparatus remain the same with Section 3.1.1 and Section 3.1.4.

3.2.2 Design. The independent variables were **S** and **V**. we controlled the factor **H** with six tested hues. The dependent variable was the depth that mapped to the target color. We set the two reference squares' colors as the extremes of the independent variable.

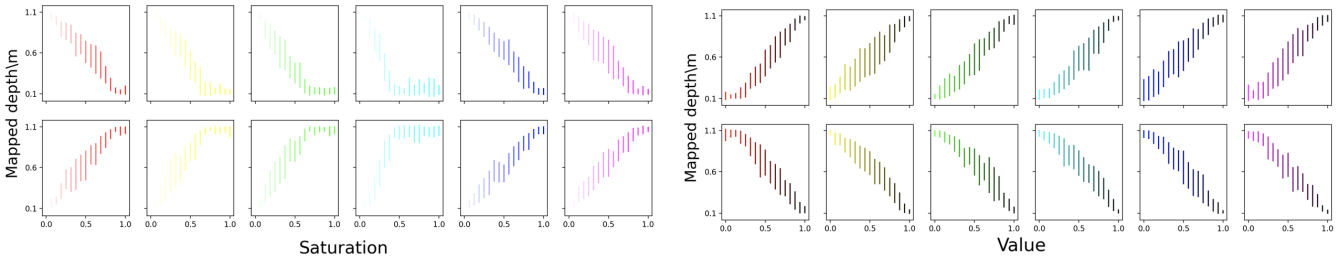

(a) (b)

Figure 4: The errorbar's position shows the average mapped depth and its length indicates the standard deviation. In the first row, the trials were conducted with the pure color reference at the front and the second row in reverse order.

For instance, if we tested **S**, one of the two references was white (**S** is 0), and the other was the pure color (**S** is 1). To test whether the front-back order of the references influences the mapping, we set reference order (whether white or the pure color is at the front) as a minor independent variable.

We separately tested **S** and **V** ranging from 0 to 1 with an interval of 1/16, which induced 17 data points on each of the six hues ($H = i/6,\ i = 1, 2, \ldots, 6$). We tested 6 (**H** values) × 2 (variables) × 2 (reference order) = 24 conditions and each participant thus completed 17 (**S/V** values) × 24 (conditions) = 408 trials in total. The order of the conditions was counter-balanced over users, and the order of the trials in each condition was randomized. The experiment was divided into four sessions with five-minute breaks between sessions. The experiment lasted around 40 minutes. Each participant received a 15 USD compensation.

3.2.3 Participants. We recruited another 24 participants (11 females, 13 males) from the local university. Participants were aged 17 to 23 with an average age of 20.12 (SD = 1.36). The average self-reported familiarity with VR score was 2.52 (SD = 1.48) with a 7-point Likert scale (1-not familiar at all, 4-neutral, 7-very familiar). All participants had normal vision and did not have color weakness or blindness.

3.2.4 Results. We calculated the average mapped depth and the standard deviation for each trial color which results are visualized in Figure 4. To compare the mappings in different reference orders, we reversed the mappings with increasing order (starting from pure color reference) by applying $depth = 1.1 - depth$ for each trial color, and calculated the Pearson correlation coefficient to measure the similarity of the paired mappings. The average coefficient of the paired depth data was higher than 0.99, which indicated that **the reversed reference order led to highly symmetric color-to-depth mappings**. Then we calculated the Pearson correlation coefficient between the **S** or **V** and the mapped depth. As shown in Figure 4a, **V linearly correlated with the mapped depth for all six hues** (all coefficients > 0.99), while **S had a linear correlation with the mapped depth for red, blue, and purple** (all coefficients > 0.99) while **the mapped depth stops increasing at a certain level of S for yellow, green, and cyan.** (all coefficients < 0.9). The standard deviation increased from 0.03 (**S** or **V** = 0) to 0.17 (**S** or **V** = 0.5) and then reduced to 0.04 (**S** or **V** = 1) in all conditions. Furthermore, when the mapped depth stops increasing at a certain level of **S** for yellow, green, and cyan, its standard deviation is also at around 0.04. This indicated that users mapped the color to depth more consistently for larger **S** and **V** and the confusion probability reaches the peak when **S** and **V** have medium values. Compared to the results with hue, participants achieved more consistent mappings with saturation and value in both reference orders.

3.3 Phase 3: Mapping (S, V) combination to Depth

Results from Phase 2 showed the potential of creating intuitive saturation/value-to-depth mappings that participants can consistently agree to. In this phase, we further investigated whether combining **S** and **V**, which essentially extends single color channels to a two-dimensional space, generates color-to-depth mappings where participants can distinguish more levels of depth. The uncertainty behind is whether the perception of **S** will be in conflict with or can supplement that of **V**.

3.3.1 Procedure and apparatus. The procedure and apparatus remain the same with Section 3.1.1 and Section 3.1.4.

3.3.2 Design. The independent variables were **S** and **V**, which both varied from 0 to 1 with an interval of 1/11. We thus sample 12 × 12 = 144 data points, as illustrated in Figure 5a. The control factor was hue with four tested hue values. We selected two hues (red and purple) where depth correlated linearly with tested **S/V** and two hues (green and cyan) where **S** behaved differently. We tested four hues (instead of all six hues in Phase 2) to reduce the task load and avoid the influence of perceptual as well as physical fatigue. Since Phase 2's results suggested that mappings with different reference orders can be converted to each other by reversing the depth value, we fixed the front reference as white and the back as black in this phase. The dependent variable was the depth that mapped to the trial color. Hence each participant needed to perform 144 (data points) × 4 (hues) = 576 trials. The order of the hues was counter-balanced with a Latin-square, and the order of the trial colors in each hue was randomized for each participant. The experiment was divided into four sessions with five-minute breaks between sessions. The experiment lasted around 60 minutes. Each participant received a 15 USD compensation for the 60 minutes experiment.

3.3.3 Participants. We recruited another 24 participants from a local university, including 11 females and 13 males. Participants were aged from 18 to 26, with an average age of 20.50 (SD = 1.62).

The average self-reported familiarity with VR score was 2.46 (SD = 1.47) with a 7-point Likert scale (1-not familiar at all, 4-neutral, 7-very familiar). All participants had normal vision and did not have color weakness or blindness.

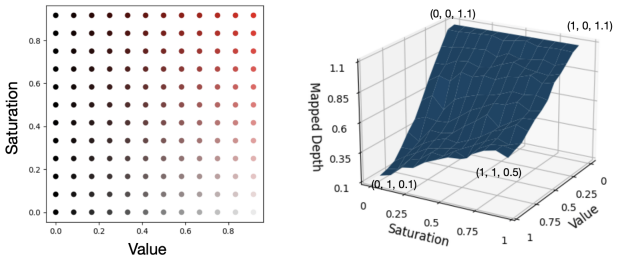

(a) (b)

Figure 5: (a) The tested data points sampled in red hue. (b) The height of each data point indicates the mapped depth. $S = 0$, $V = 1$ (white) is mapped to 0.1 depth. $V = 0$ (black) is mapped to 1.1 depth.

3.3.4 Results. We interpolated the average mapped depths based on the collected sample points and plotted the results for red hue as an example in Figure 5b. Please refer to supplementary material for the results of other hues. Observing from Figure 5b, the interpolation results formed a surface close to the inclined plane which indicated that the mapped depth was affected by **S** and **V** approximately linearly. The coefficient of multiple correlation [2] on the four hues were all over 0.96, which verified this finding. We conducted Repeated-Measures ANOVA with Greenhouse-Geisser-corrected on the results. Analysis results showed that **S** and **V** had a significant interaction effect for green ($F_{(121,2783)} = 2.65$, $p = 0.01$) and cyan ($F_{(121,2783)} = 3.18$, $p = 0.001$) while no significant interaction effect for red ($F_{(121,2783)} = 2.10$, $p > 0.05$) and purple ($F_{(121,2783)} = 1.36$, $p > 0.05$). This indicated that **V** affected the **S**'s influence on the mapped depth and made it become more linear with the reduction of **V** for green and cyan.

4 A COMPUTATIONAL MODEL TO GENERATE COLOR-TO-DEPTH MAPPINGS

4.1 Trade-off between confusion probability and depth resolution

A color-to-depth mapping consists of paired colors and depths, so that users can infer or recognize the depth with the color as the cue. There exists a trade-off between the confusion probability and depth resolution, as a larger number of (color, depth) pairs potentially can support the distinguishability of more levels of depth while as the selected colors become more crowded in the color space, the probability of users confusing with the colors also becomes higher. For example, two colors representing two depths could express one-bit information. However, if users tend to map the same depth to these two colors, or they could not distinguish between two depth levels with the help of color cues, we lose the color-to-depth mapping's resolution.

The results of the user studies showed that participants might map a range of depths to the same trial color, which followed a normal distribution ($p > 0.05$) for all tested colors suggested by Shapiro-Wilk tests. As the depth range mapped to two colors may overlap with each other (as illustrated in Figure 6a), a color-to-depth mapping containing the two colors will cause confusions. We used the overlapping area of the two normal distributions to calculate the confusion probability of two colors. We calculate the entire mapping's average confusion probability as the mean of the confusion probability between every two neighboring (color, depth) pairs and its depth resolution as the number of pairs it contains.

Based on the collected data in the previous studies, we set up a model for generating color-to-depth mappings that satisfy interaction requirements.

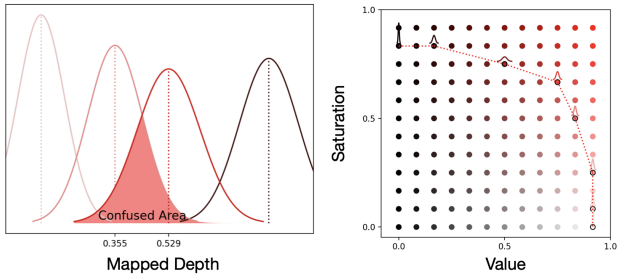

(a) (b)

Figure 6: (a) An example of the distribution of the mapped depths for four color cues. The overlapping area between two distributions indicates the confusion probability. (b) The longest path found with Algorithm 1 that satisfied the requirements and the constraints. The mapped depth distribution of selected point is plotted above each point.

4.2 Generating color-to-depth mappings

We set up a model that takes in various constraints and requirements, and generates applicable color-to-depth mappings. The model allows selecting the starting and ending reference colors *(input 1), which regulate a color range that the selected colors will not be less than the starting color or more than the ending color in saturation or value. And the model takes in the required confusion level (input 2)* which is the upper limit of the predicted probability of users confusing any of the two colors. We ensured the depth represented by the color should change monotonously with the color's saturation and value *(constraint 1)*. To enhance the mapping's resolution, it should contain as many as possible (color, depth) pairs *(constraint 2)*.

Under the requirement of confusion probability between any two colors in the mapping, the whole mapping's average confusion probability should be minimized *(constraint 3)*.

Algorithm 1 illustrates the algorithm procedure. We firstly interpolated the mean and standard deviation of the colors tested in Section 3.3 and get the $dmean_H(s, v)$ and $dstd_H(s, v)$ function. Then with these two functions, we resampled the color space with a resolution of 101 ×101. We had tested the resolution of 26 × 26, 51 × 51, 101 × 101, and 201 × 201. The last two had the same results, and we thought that the resampling data point could restore the function accurately with a certain resolution. So we selected the

Algorithm 1 Generate a color-to-depth mapping with given inputs and constraints

Initialize *MaxLength* and *PrevColor* as a 101×101 matrix
For s = 0, s <= 100, s = s + 1
    For v = 100, v >= 0, v = v - 1 {The search starts from white and ends at black.}
        MaxLength[s][v] = 0 {Initial the size of the biggest color-to-depth mapping that ends at (s, v).}
        For *prev_s* = 0, *prev_s* < s, *prev_s* = *prev_s* + 1
            For *prev_v* = 100, *prev_v* > v, *prev_v* = *prev_v* - 1
                If $dmean_{H,\,(s,v)} - dstd_{H,\,(s,v)} > dmean_{H,\,(prev\_s,\,prev\_v)} + dstd_{H,\,(prev\_s,\,prev\_v)}$ and *MaxLength*[s][v] ≤ *MaxLength*[*prev_s*][*prev_v*] + 1 {Check if it satisfies the confusion probability} requirement and if this previous color could produce a new longest path.
                    PrevColor[s][v] = (*prev_s*, *prev_v*), *MaxLength*[s][v] = *MaxLength*[*prev_s*][*prev_v*] + 1 {Update} the size and the previous color of the biggest color-to-depth mapping that ends at (s, v).
$\{M\}$ = {{(H, s', v', $dmean'$, $dstd'$)}| (s', v') is in *PrevColor*[s][v] which (s, v) makes *MaxLength*[s][v] is the biggest} {Leverage *PrevColor* to find out the points on every longest path and record with the form of $\{(H, s, v, dmean, dstd)\}$.}
Return $\arg\min_{M}(p_M = \frac{\sum_{M=1} P(dmean'+dstd'<dmean-dstd)}{\text{M' size}})$ {Return the color-to-depth mapping with the least confusion probability. $P(dmean' + dstd' < dmean - dstd)$ is the overlapping area between two contiguous colors in M.}

101 × 101 resolution in our algorithm. With this preparation, we developed a search algorithm to determine the color-to-depth mappings that satisfied the requirements. We convert this problem to a searching problem to find the longest path in the resampling data points. We initialized the data structure for the following algorithm *(Step 1)*. *MaxLength*[s][v] saves the length of the longest path that ends at (s, v), and *PrevColor*[s][v] saves the last color before (s, v) in the longest path. Then the search started from white (saturation is 0, value is 1) and ended at black (saturation is 1, value is 0) *(Step 2 & 3)*. After updating the iterator, we set the longest path length as 1 to search for the local optimal solution *Step 4*. Then we search all of the previous colors ranging from white to the current color *(Step 5 & 6)* to update the longest path length ends at the current point *(Step 7 & 8)*. After the search, we could have multiple longest paths with the same length. Then we found out which colors these paths contained with recorded data *(Step 9)*. Finally, we calculated the confusion probability of the whole mapping and selected the one with the least confusion probability *(Step 10)*. Please refer to the supplementary material for the detailed version of the algorithm.

We ran the algorithm 1 on the results of red hue in Section 3.3, with the starting color of (S = 0, V = 0), ending color of (S = 1, V = 1), a threshold of confusion probability as 31.8%, which corresponds to one standard deviation in normal distributions. As a result, we obtained a color-to-depth mapping with the maximized 8 (color, depth) pairs and minimized confusion probability of 23.8% on average. The mapping is visualized in Figure 6b. We also applied the same algorithm on the results of single **S** channel and **V** channel in Section 3.2, with starting colors of (S = 0, V = 1) and (S = 1, V = 0), ending color of (S = 1, V = 1). The results showed that only altering **S** or **V** supports for distinguishing at most four depth levels, which confirmed that the combination of **S** and **V** provides color-to-depth mappings with better depth resolution than either channel.

5 EVALUATION OF THE COLOR-TO-DEPTH MAPPING

We conducted an user study on a mid-air sketching task to evaluate whether the color-to-depth mapping generated by the algorithm in Section 4.2 could enhance participants' depth perception in VR interaction tasks.

5.1 Design

Participants were asked to observe a target shape and sketch to reproduce the shape beside it. In this process, we can study whether applying the mapping can facilitate the observation of the *target* shape and/or the user's movement control. We also wanted to investigate whether the mapping could improve the sketching performance on *2D and/or 3D* shapes. Thus participants were asked to complete the study in 2 output levels (color-to-depth mapping *vs.* single colored target) × 2 input levels (color-to-depth mapping *vs.* single colored strokes) × 2 types of shapes (2D *vs.* 3D) = 8 conditions. Table 1 listed these conditions and the factors. We designed a within-subject study with independent variables augmenting technique (*NN*, *CN*, *NC*, *CC*) and shapes (*2D*, *3D*). In this experiment, we rendered the targets and sketching strokes in pure black as a baseline. The underlying consideration was that, to our knowledge, there is no commonly agreed color-to-depth mapping in current VR sketching applications for comparison, so the pure color baseline serves as a neutral reference to help evaluate the proposed mapping's performance.

The trial target shapes are illustrated in Figure 7a. To test the sketching accuracy in a 3D space, we rotated the 2D and 3D shapes on the dimensions of roll, pitch, and yaw with an interval of 45 degrees. After removing the repeated ones, we ended up with 23 2D and 12 3D distinctive targets. Each participant thus need to perform $4 \times 23 + 4 \times 12 = 140$ trials. We counterbalanced the order of the eight conditions with a Latin-square, and the order of target shapes in each condition was randomized for each participant. After completing trials in each condition, the participant took a three-minute break and answered a questionnaire based on a 7-point Likert scale (1: strongly disagree; 4: neutral; 7: strongly agree) in five aspects:

- *Easiness*: It is easy to sketch with the technique.
- *Confidence*: I can draw the shapes accurately.
- *Mental workload*: I feel mentally tired.

- *Preference*: I like the color-to-depth augmentation.
- *Willingness*: I am willing to use the sketching technique with the color-to-depth augmentation.

Since there were no color cues in *NN2* and *NN3* conditions, participants were not asked to answer the last two questions in these two conditions. As for the quantitative metrics, we evaluated the user's task completion time and error of orientation, size, similarity, and depth. Each participant received a 15 USD compensation for the 60 minutes experiment.

Condition	Target	Sketch	Shape
NN2	None	None	2D
CN2	Color-to-depth	None	2D
NC2	None	Color-to-depth	2D
CC2	Color-to-depth	Color-to-depth	2D
NN3	None	None	3D
CN3	Color-to-depth	None	3D
NC3	None	Color-to-depth	3D
CC3	Color-to-depth	Color-to-depth	3D

Table 1: The factorial design of the eight conditions that we tested in the experiment.

5.2 Procedure

To control the relative observation angle, we asked the participant to sit on a chair during the experiment. After recording the participant's personal information, we conducted a warm-up session to help the participant get familiarized with the experiment. Pressing A on the controller started a trial and the target shape appeared. Then the participant could draw strokes in the virtual space by pressing the index finger trigger on the controller. Pressing B on the controller cleared the VR scene and ended the current trial. Participants were allowed to put their arms down during the trials to reduce the influence of physical fatigue.

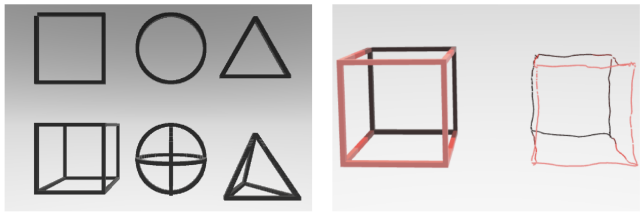

(a) (b)

Figure 7: (a) The 2D and 3D target shapes tested in the evaluation. (b) An example of the CC3 condition: left is the color-augmented target and right is the color-augmented sketch. The colors at different depths were determined by the color-to-depth mapping generated in Section 4.

5.3 Apparatus

We implemented the experiment platform using Unity 2019 and ran it on the Oculus Quest 2 with Oculus Link connected to a desktop so that the experimenter could observe the participant's behaviors in VR. The tracking frequency of the handheld controller was 60Hz, and the Oculus Quest2 display had a 30Hz refresh rate. The target shapes were shown at 10 cm beneath the user's head,10 cm towards the left, and from 20 cm to 40 cm from the user in depth, which were within their arms' reach and used in other sketch research [5]. We applied the red color-to-depth mapping in this range as well. The length of the target shape's side (diameter for ring and sphere) was 8cm. We conducted the experiment with a white background to control the influence of the virtual background. Figure 7b illustrated the virtual scene in the experiment.

5.4 Participants

We recruited 16 participants from a local university, including 8 females and 8 males. Participants' ages ranged from 21 to 24, with an average of 21.94 (SD = 0.99). The average self-reported familiarity with VR score was 3.69 with a standard deviation of 1.54 with a 7-point Likert scale (1: strongly disagree; 4: neutral; 7: strongly agree). All participants had normal vision and did not have color weakness or blindness.

5.5 Results

We conducted Repeated-Measures ANOVA with Bonferroni-corrected post-hoc T-tests on the quantitative metrics. As for the qualitative results, we conducted a non-parametric analysis of variance based on the Aligned Rank Transform with the post-hoc t-tests.

We used the **completion time**, **orientation error**, **size error**, **similarity error** and **depth error** to comprehensively evaluate a 3D sketch's accuracy and depth specifically. We calculated the duration **completion time** from the user started to observe the pattern till he finished the task. For 2D shapes, we used the least square error to estimate a plane that best fits the strokes and calculated the **orientation error** between the target shape and the plane. As for 3D shapes, we estimated a plane for every surface in a shape and calculated the overall **orientation error**. After revising the orientation error, we calculated the **size error** by computing the percentage error of the length of the diagonal. The length of the user-drawn diagonal stroke was estimated by the average distance of 10 furthest apart pairs of points to avoid the outliers' influence. The **similarity error** was then calculated on sketches with corrected orientation and size. The **similarity error** was represented by the overall space distance between points in a target-sketch mapping generated by a DTW [11] algorithm. With the mapping results given by Dynamic Time Warping (DTW [67]) algorithm, we calculated the overall **depth error** between the targets and the raw sketches without revisions to investigate the color-to-depth mapping's influence on the depth perception.

5.5.1 Completion time. Participants did not use more time to sketch with the augmented input and/or output while they spent more time on 3D shapes. Statistical analysis results showed that only *2D/3D* had a significant effect on completion time error ($F_{(1,15)} = 335.06$, $p < 0.001$). Pair-wise results showed that *CC2* ($AVG = 9.13$, $SD = 5.76$) had a larger completion time than *NN2* ($AVG = 7.05$, $SD = 4.02$, $t = 4.38$, $p = 0.001$), *CN2* ($AVG = 6.77$, $SD = 3.25$, $t = 5.44$, $p < 0.001$), *NC2* ($AVG = 6.83$, $SD = 3.77$, $t = 4.82$, $p < 0.001$). These results indicated that the user would compare his augmented sketch to the augmented target on 2D shapes. However,

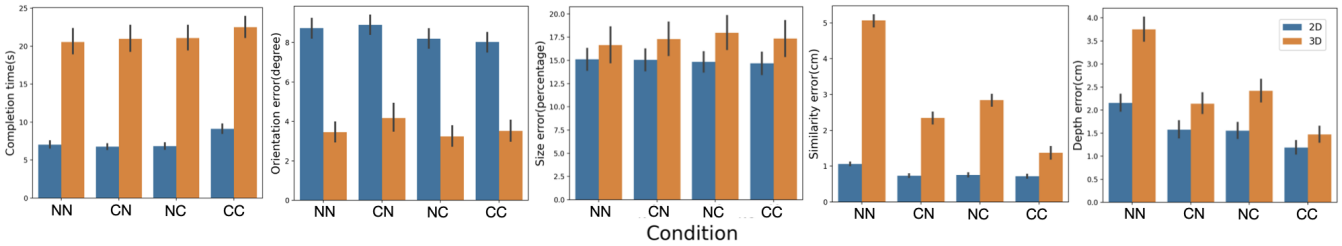

Figure 8: Quantitative results on the completion time, orientation error, size error, similarity error, and depth error. 3D and 2D sketch results are visualized with blue and orange colors.

the completion time on 3D shapes has no significant difference in the four conditions.

5.5.2 Orientation error. Participants performed similarly on orientation with or without color cues while the orientation error on 3D shapes was significantly less. Statistical analysis results showed that only *2D/3D* had a significant effect on orientation error ($F_{(1,15)}$ = 138.42, $p < 0.001$) and there was no interaction effect. The 3D shapes' orientation error is significantly smaller since the user could perceive the virtual object's space orientation better by leveraging the spatial relationship of different surfaces.

5.5.3 Size error. The color cues did not significantly influence the sketch's size error while 3D shapes had a larger size error. Results showed that only *2D/3D* had a significant effect on size error ($F_{(1,15)}$ = 16.23, $p < 0.001$) and there was no interaction effect.

5.5.4 Similarity error. Participants could draw the shapes more similar to the target shapes with augmented targets and/or augmented sketches while the 3D shape had a larger similarity error than 2D. Results showed that there was a significant effect on similarity error of *target* ($F_{(1,15)}$ = 96.97, $p < 0.001$), *sketch* ($F_{(1,15)}$ = 53.78, $p < 0.001$), and *2D/3D* ($F_{(1,15)}$ = 252.64, $p < 0.001$). Pair-wise results showed that *NN2* ($AVG = 1.06$, $SD = 0.14$) had a larger similarity error than *CN2* ($AVG = 0.73$, $SD = 0.12$, $t = 7.80$, $p < 0.001$), *NC2* ($AVG = 0.76$, $SD = 0.14$, $t = 7.03$, $p < 0.001$), *CC2* ($AVG = 0.71$, $SD = 0.15$, $t = 6.71$, $p < 0.001$). This indicated that augmenting either the input or the output could improve the similarity error on 2D shapes. While on 3D shapes, *NN3* ($AVG = 5.07$, $SD = 0.70$) had a larger similarity error than *CN3* ($AVG = 2.34$, $SD = 1.02$, $t = 8.15$, $p < 0.001$), *NC3* ($AVG = 2.84$, $SD = 1.08$, $t = 6.75$, $p < 0.001$), *CC3* ($AVG = 1.37$, $SD = 0.94$, $t = 11.99$, $p < 0.001$). And *CC3* had a less similarity error than both *CN3* ($t = 2.94$, $p = 0.01$) and *NC3* ($t = 4.51$, $p < 0.001$). Compared to *NN3* ($AVG = 5.07$), the similarity error reduced by 72.98% in *CC3* ($AVG = 1.37$). These results indicated that the color cues could improve the similarity error and the improvement was more significant when both the target and the sketch were augmented.

5.5.5 Depth error. Participants could perceive and control the virtual sketch's depth better with augmented target and/or augmented sketches while the 3D shape had a larger depth error than 2D. Results showed that there was a significant effect on depth error of *target*($F_{(1,15)}$ = 76.79, $p < 0.001$), *sketch*($F_{(1,15)}$ = 45.23, $p < 0.001$), and *2D/3D*($F_{(1,15)}$ = 21.12, $p < 0.001$). Pair-wise results showed that *NN2*($AVG = 2.15$, $SD = 0.83$) had a larger similarity error than *CN2* ($AVG = 1.57$, $SD = 0.78$, $t = 2.46$, $p < 0.05$), *NC2*($AVG = 1.55$, $SD = 0.82$, $t = 2.35$, $p < 0.05$), *CC2*($AVG = 1.19$, $SD = 0.93$, $t = 3.02$, $p < 0.01$). While *CN2*, *NC2*, and *CC2* don't have significant difference with each other ($p > 0.05$), this indicated that augmenting only the input or the output could improve the depth on 2D shapes. On 3D shapes, *NN3* ($AVG = 3.75$, $SD = 0.47$) also had a larger similarity error than *CN3* ($AVG = 2.14$, $SD = 0.69$, $t = 6.80$, $p < 0.001$), *NC3* ($AVG = 2.41$, $SD = 0.98$, $t = 4.33$, $p = 0.001$), *CC3* ($AVG = 1.47$, $SD = 0.73$, $t = 10.30$, $p < 0.001$). Furthermore, augmenting the input and output simultaneously(*CC3*) could significantly improve the depth error compared to only augmenting the input(*NC3* ($t = 2.46$, $p < 0.05$)) or the output(*CN3* ($t = 2.97$, $p = 0.01$)). The depth error reduced by 72.98% in *CC3* ($AVG = 1.47$) compared to *NN3* ($AVG = 3.75$), This indicated that our color-to-depth mapping could improve the perception and control of the virtual object's depth and the improvement was more significant when both the target and the sketch were augmented by the color-to-depth mapping.

5.5.6 Easiness. Participants felt easier to sketch both 2D and 3D shapes with color cues. Results indicated statistically significant effect on *Easiness* of *target*($F_{(1,105)}$ = 28.32, $p < 0.001$), *sketch*($F_{(1,105)}$ = 38.50, $p < 0.001$), and *2D/3D*($F_{(1,105)}$ = 23.50, $p < 0.001$). Post-hoc tests results showed that participants felt easier to sketch in *CC2*($AVG = 5.35$, $SD = 0.90$) compared to *NN2* ($AVG = 4.00$, $SD = 1.00$, $t = -4.93$, $p < 0.001$) on 2D shapes. While on 3D shapes, *CC3*($AVG = 5.19$, $SD = 0.63$) had significant difference with *NN3*($AVG = 3.25$, $SD = 0.90$, $t = -6.76$, $p < 0.001$), *CN3*($AVG = 3.63$, $SD = 1.27$, $t = -5.40$, $p < 0.001$), and *NC3*($AVG = 3.75$, $SD = 1.09$, $t = -5.16$, $p < 0.001$).

5.5.7 Confidence. Participants were more confident with their sketch's accuracy with color cues on both 2D and 3D shapes while they had more confidence on 2D shapes. Results indicated statistically significant effect on *Confidence* of *target*($F_{(1,105)}$ = 40.01, $p < 0.001$), *sketch*($F_{(1,105)}$ = 79.70, $p < 0.001$), and *2D/3D*($F_{(1,105)}$ = 37.36, $p < 0.001$). Post-hoc tests results showed that participants were more confident with color cues on the sketch strokes since the ratings on *CC2*($AVG = 5.25$, $SD = 0.66$) had a significant difference with *NN2*($AVG = 3.63$, $SD = 0.93$, $t = -5.99$, $p < 0.001$). The conclusion remained the same on 3D shapes since the ratings on *CC3*($AVG = 4.75$, $SD = 0.75$) had a significant difference with *NN3*($AVG = 2.69$, $SD = 0.68$, $t = -7.85$, $p < 0.001$ and *CN3*($AVG = 3.06$, $SD = 0.75$, $t = -6.52$, $p < 0.001$.

Figure 9: Qualitative results on the easiness, confidence, mental workload, preference, and willingness.

5.5.8 Mental workload. Participants did not feel more mentally tired with color cues on both 2D and 3D shapes. Results indicated statistically significant effect on *Mental workload* of *2D/3D* ($F_{(1,105)} = 8.86$, $p < 0.01$). Post-hoc tests showed that no significant difference exists.

5.5.9 Preference. Participants preferred augmented targets and augmented sketches on both 2D shapes and 3D shapes. Results indicated statistically significant effect on *Preference* of *sketch* ($F_{(1,105)} = 14.28$, $p < 0.001$), and *2D/3D* ($F_{(1,105)} = 19.72$, $p < 0.001$). Post-hoc tests results showed significant difference on the ratings between: *CN2* ($AVG = 4.24$, $SD = 0.86$) and *CC2* ($AVG = 5.38$, $SD = 0.86$, $t = -3.37$, $p < 0.05$, *CN3* ($AVG = 3.44$, $SD = 1.25$) and *CC3* ($AVG = 5.13$, $SD = 0.93$, $t = -4.99$, $p < 0.001$).

5.5.10 Willingness. Participants are willing to use augmented targets and augmented sketches on both 2D shapes and 3D shapes. Results indicated statistically significant effect on *Willingness* of *sketch* ($F_{(1,105)} = 26.06$, $p < 0.001$), and *2D/3D* ($F_{(1,105)} = 12.79$, $p < 0.01$). Post-hoc tests results showed significant difference on the ratings between: *CN2* ($AVG = 4.06$, $SD = 1.09$) and *CC2* ($AVG = 5.56$, $SD = 0.86$, $t = -5.10$, $p < 0.001$, *CN3* ($AVG = 3.25$, $SD = 1.19$) and *CC3* ($AVG = 5.38$, $SD = 0.93$, $t = -6.64$, $p < 0.00$).

6 APPLICATIONS

To demonstrate how the generated color-to-depth mappings can be beneficial, we developed four example applications, as shown in Figure 10. The first three built on previous research [16, 18, 22], including performing mid-air gestures, arranging UI layouts, and scientific data visualization. The last one illustrates the potential of applying the mappings in Augmented Reality (AR) scenarios and enabling the switch between depth perspectives. The mappings applied in these applications are all generated with the proposed model on the data that we have collected. We believe that with extra efforts in data collection, similar mappings between depth and other attributes, for instance contrast and transparency, can be generated which might suit different applications better.

6.1 Improving accuracy of performing mid-air gestures in VR

Similar to providing target shapes in the sketching task that we tested, providing visual guides of the mid-air gestures is a commonly applied method to reduce the user's efforts in recalling the gestures. Fennedy et al. proposed to use dynamic guides to help users perform the gestures by visualizing possible 3D gestures in VR [22]. At the start, gesture strokes of different commands are visualized with different hues. As the user gradually follows the visual guide to complete the target stroke, the system filters out the less probable gestures by comparing the user's current stroke and the candidates. In this process, the more accurately the user follows the stroke, the more efficiently the system can filter out non-target strokes and recognize the target. We expect that augmenting the gesture strokes with color-to-depth mappings that alter saturation and value can help users make sense of the 3D structure of the strokes (as proved in the evaluation) and thus follow them accurately. We thus implemented, as shown in Figure 10a, a color-to-depth mapping from white to black which indicates the depth of each stroke and adapts accordingly as the user follows the stroke.

6.2 Facilitating user interface arrangement

Suggested by SemanticAdapt [16], users have a need to arrange UI elements into grouped patterns, including rows, columns, or grids, and place them at different depth layers according to their interaction priority levels. For example, the user may want to place the social applications that they frequently interact with at the nearest layer, and several documents that they read but do not necessarily touch in the middle layer, and other applications like weather and shop list in the furthest layer. To facilitate this process, we implemented a mode-switch function that replaces the original color of the elements with a color-to-depth mapping, and users can accurately group sets of elements to be at different depth levels. After they are satisfied with the layout, they can switch back from the colored mode. As Figure 10b illustrated, initially multiple virtual elements (e.g., virtual icons, web browsers, weather widgets) were laid out in a default manner. Then the user could leverage the color-to-depth mapping to place these virtual interfaces at different layers of depth to facilitate reading and interactions.

6.3 Enhancing 3D data visualization

Data visualization is essential to helping users understand data. Immersive virtual reality can help researchers to perceive and understand data in a 3d space [18, 23]. We propose to augment the visualization by altering the saturation and value of the colors of the data points to infer their depths. Figure 10c shows an example with four types of data points, colored by different hues. In this case, we could apply four separate color-to-depth mappings to the four groups and adapts the saturation and value in response to the change of the user's observation perspective in a user-centric reference frame. In this manner, the user can further observe the distribution of the data points on the depth axis and make sense of the spatial relationship between the data points. As suggested in MRAT [54], we allow users to further zoom into a certain group and we can adapt the color-to-depth mapping accordingly for clearer observation.

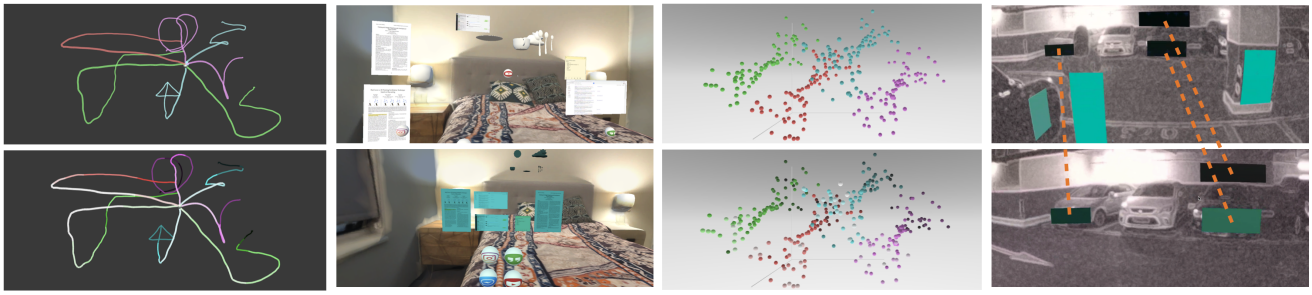

(a) (b) (c) (d)

Figure 10: (a) Augmented OctoPocus [22]: The mid-air gesture guidance is colored with various S and V to improve tracing accuracy. (b) Facilitating virtual elements arrangement: The virtual elements are augmented to help users precisely place elements at different depth layers. (c) Enhancing 3D data visualization: We augment the data visualization to hint at the spatial relationship between the data points. (d) Enhancing real world depth perception: We use the color-to-depth mapping to hint at the physical objects' depth to facilitate the user's observation.

6.4 Enhancing real world depth perception

Depth misperception not only exists in virtual space but also in the real world. Users can have problems deciding the physical depth in various scenarios, e.g., driving, reaching objects, and navigating. We thus developed a demonstration that facilitates the user's observation of physical objects' depth in real world by augmenting the physical objects with a color-to-depth mapping. We used the pass-through function of Quest 2 headset to develop an AR application as illustrated in Figure 10d. The figure shows a parking lot with several cars, pillars and a pedestrian in the scene augmented with a color-to-depth mapping. It would be hard to determine the distance to these objects for the drivers in such a narrow and small space. As computer vision techniques (e.g., SLAM) would enable us to measure the distance from the camera to objects, we can render color effects on the physical objects to notify the users about the depth information. In our current implementation, we did not integrate SLAM algorithms, as we manually placed the virtual planes to the position of the physical object and then calculated the relative depth in real time. In this scenario, it is interesting that the relative depth between the car and the obstacles is the key information to present, so we actually apply the mapping in a car-centric reference frame. We consider that closer objects are more dangerous to users and make them brighter and bigger while further ones are darker and smaller. We recognize that it is an important future work to explore applying color-to-depth mappings from different perspectives. In addition, we expect that color-to-depth mappings may be more useful for users with low vision to gain a better sense of the obstacles in their way as they may have challenges obtaining other precise depth cues.

7 DISCUSSION

This paper investigated how users map the color space to the depth axis through several user experiments. Based on the results, we devised a computational model able to generate color-to-depth mappings that fulfill various constraints and requirements. We evaluated the generated mapping in a sketching task compared to single-colored baseline conditions. In this section, we discuss ways of extending the mappings and the limitations of our work.

7.1 Mapping depth to other channels than color

Other than color, it is also common practice to use contrast, opacity, blurriness, and other rendering attributes of objects to deliver depth information. Even for color, there are multiple kinds of models to represent a color (e.g., RGB, HSL, CDIE). As we discussed in Section 6, other visual channels may fits certain scenarios better than color, and we recognize it worthwhile to explore these channels in the future. We expect the research methodology presented in this paper could also be leveraged in the research of other channels or other representations of color. For instance, distance fog [78] is another widely used technique to present depth information by using fog to change objects' contrast and opacity in virtual scenes. Similar to color-to-depth mappings, using fog to render depth has a trade-off between the number of fog layers and confusion probability. If the fog has lots of layers, users will also be confused about the presented depth information. Researchers thus could leverage our methodology to investigate the relationship between the distance fog and the user perceiving depth.

7.2 Adjustable inputs, constraints and usages of the model

As the study results in Section 3 show, the optimal color-to-depth mappings that provide the most depth levels with the least confusion level are mostly non-linear, and they cannot be generated through simple interpolation. Therefore, we presented an algorithm that took in a given confusion probability and other constraints and then outputs a color-to-depth mapping. Except for the proposed ones, the constraints can also be varied to satisfy different needs, such as changing the starting and ending color to meet the user's personal preference or strengthening the requirements for confusion probability for scenarios very sensitive to depth perception, e.g., the driving application. Moreover, we could also use the model reversely to calculate the confusion probability when given a color-to-depth mapping. With Section 3 results, we could interpolate the sampled data points and calculate the confusion probability for arbitrary saturation and value on the hue. This could

help other researchers or designers who would like to know if their color-to-depth mapping is confusing or not.

7.3 Additional support for mode switch and input augmentation

We recognized there could be potential issues with using the mappings in practical scenarios. It is common for users to color their sketches for aesthetic and other purposes while if the color-to-depth mapping is applied, the original color could affect the presentation of depth information. Furthermore, if the mapping is applied in driving discussed in Section 6.4, the environment color could be essential for users, such as the traffic lights. To solve these issues, we could apply a mode switch in practical use. Users could easily switch to the color mode to observe the object's depth and switch back to the normal mode when color is not needed. We could also design other augmentation techniques to show our color augmentation and the object's original color simultaneously, e.g., adding colored outlines around the object. And in sketch application, we could also combine the color-to-depth mappings with other auto-corrected techniques [83, 84] to improve the sketching's accuracy and aesthetics.

7.4 Limitations and future work

In our study, all participants had normal vision and did not have color weakness or blindness. In future work, it would be interesting to explore how to best adapt our computational model to support different types of color blindness and further investigate possible applications of our work to enhance accessibility of VR interfaces (e.g., developing new lenses for the SeeingVR [85] toolkit).

Since environmental factors (e.g., background, lightness), and the mental and physical state of users (e.g., digital eye strain [24]) can also influence the user's color perception [49], we will evaluate proposed mappings in more complex and realistic scenarios in the future.

In this paper, we investigate the color-to-depth mapping within a reachable distance in which most interactions happen. We also generated color-to-depth mappings that worked well in this most frequently used range. However, the depth perception issue also exists for further objects. Moreover, the objects may not be right ahead of the user and the color-to-depth mapping can be affected the observation angle. Our research methodology can be extended to other depth ranges and observation angles in future research.

In Section 3, we collected data from a group of users so that the model built on it could be extendable to the general population. However, we believe with more data collected with the same user, the model can also be adapted for personalization purpose. We investigated and evaluated the color-to-depth mappings while users sat in the chair with a static pose and observed the virtual objects. However, if the user is freely moving in the virtual space, mapping colors to ego-centric or world-anchored depth might result in different user experiences. While our color-to-depth mapping can be leveraged to render both kinds, we will further investigate the differences between rendering ego-centric and world-anchored depths in the future.

In Section 5, we evaluated a discrete color-to-depth range mapping since we collected data on discrete colors. If we used the discrete results to generate a continuous mapping, the mapping's confusion probability and expressivity may be different. Future research should investigate this further and can leverage our results to generate continuous color-to-depth mappings. Besides, we chose a pure color as the baseline method instead of existing color mappings. Our consideration is to use a neutral reference to avoid cherry-picking as no standard mapping is commonly agreed for the task. We acknowledge that it remains unclear whether and how our mappings outperforms the existing mappings in various tasks and thus more comparisons are required as future work.

8 CONCLUSION

This paper investigates how to use color as a cue to improve the user's depth perception in VR. In approaching this, we studied how users map the 3D color space to the depth axis. We conducted three user studies to explore each color's representing depth and confusion probability with other colors. With the results, we constructed a computational model to generate color-to-depth mappings with a given confusion probability and several constraints. We then generated a red color-to-depth mapping and conducted a user study to evaluate it on a sketch application. Results showed that the color-to-depth mapping could significantly improve the sketch's similarity and depth accuracy. Users were more confident in their accuracy while did not feel more mentally tired with color cues. We demonstrated the usability of the color-to-depth mappings in four applications that augment the user's observation and motion control.

ACKNOWLEDGMENTS

This work is supported by the National Key R&D Program of China under Grant No.2020AAA0105200, the Natural Science Foundation of China under Grant No.62102221, No.62132010, No.62002198, Beijing Academy of Artificial Intelligence (BAAI), Beijing Key Lab of Networked Multimedia, and the Institute for Guo Qiang and Institute for Artificial Intelligence, Tsinghua University.

REFERENCES

[1] 2022. 15 Ways to Draw the Illusion of Depth. https://ranartblog.com/blogarticle20.html. [Online; accessed 22-March-2022].
[2] Herve Abdi. 2007. Multiple correlation coefficient. *Encyclopedia of measurement and statistics* 648 (2007), 651.
[3] Anastasios Nikolas Angelopoulos, Hossein Ameri, Debbie Mitra, and Mark Humayun. 2019. Enhanced depth navigation through augmented reality depth mapping in patients with low vision. *Scientific reports* 9, 1 (2019), 1–10.
[4] Claudia Armbrüster, Marc Wolter, Torsten W. Kuhlen, Will Spijkers, and Bruno Fimm. 2008. Depth Perception in Virtual Reality: Distance Estimations in Peri- and Extrapersonal Space. *Cyberpsychology Behav. Soc. Netw.* 11, 1 (2008), 9–15. https://doi.org/10.1089/cpb.2007.9935
[5] Rahul Arora, Rubaiat Habib Kazi, Fraser Anderson, Tovi Grossman, Karan Singh, and George W. Fitzmaurice. 2017. Experimental Evaluation of Sketching on Surfaces in VR. In *Proceedings of the 2017 CHI Conference on Human Factors in Computing Systems, Denver, CO, USA, May 06-11, 2017*, Gloria Mark, Susan R. Fussell, Cliff Lampe, m. c. schraefel, Juan Pablo Hourcade, Caroline Appert, and Daniel Wigdor (Eds.). ACM, 5643–5654. https://doi.org/10.1145/3025453.3025474
[6] Reynold J. Bailey, Cindy Grimm, and Christopher Davoli. 2006. The effect of warm and cool object colors on depth ordering. In *International Conference on Computer Graphics and Interactive Techniques, SIGGRAPH 2006, Boston, Massachusetts, USA, July 30 - August 3, 2006, Research Posters*, John W. Finnegan and Mike McGrath (Eds.). ACM, 195. https://doi.org/10.1145/1179622.1179845
[7] Reynold J Bailey, Cindy M Grimm, Chris Davoli, et al. 2006. The real effect of warm-cool colors. (2006).
[8] Lyn Bartram, Abhisekh Patra, and Maureen C. Stone. 2017. Affective Color in Visualization. In *Proceedings of the 2017 CHI Conference on Human Factors in*

Computing Systems, Denver, CO, USA, May 06-11, 2017, Gloria Mark, Susan R. Fussell, Cliff Lampe, m. c. schraefel, Juan Pablo Hourcade, Caroline Appert, and Daniel Wigdor (Eds.). ACM, 1364–1374. https://doi.org/10.1145/3025453.3026041

[9] Sebastiano Battiato, Salvatore Curti, Marco La Cascia, Marcello Tortora, and Emiliano Scordato. 2004. Depth map generation by image classification. In *Proceedings of the Conference on Three-Dimensional Image Capture and Applications VI, San Jose, CA, USA, January 18, 2004 (SPIE Proceedings, Vol. 5302)*, Brian D. Corner, Peng Li, and Roy P. Pargas (Eds.). SPIE, 95–104. https://doi.org/10.1117/12.526634

[10] Joseph A Bellizzi and Robert E Hite. 1992. Environmental color, consumer feelings, and purchase likelihood. *Psychology & marketing* 9, 5 (1992), 347–363.

[11] Donald J Berndt and James Clifford. 1994. Using dynamic time warping to find patterns in time series.. In *KDD workshop*, Vol. 10. Seattle, WA, USA:, 359–370.

[12] Matthias Berning, Daniel Kleinert, Till Riedel, and Michael Beigl. 2014. A study of depth perception in hand-held augmented reality using autostereoscopic displays. In *IEEE International Symposium on Mixed and Augmented Reality, ISMAR 2014, Munich, Germany, September 10-12, 2014*. IEEE Computer Society, 93–98. https://doi.org/10.1109/ISMAR.2014.6948413

[13] David Borland and Russell M. Taylor II. 2007. Rainbow Color Map (Still) Considered Harmful. *IEEE Computer Graphics and Applications* 27, 2 (2007), 14–17. https://doi.org/10.1109/MCG.2007.46

[14] Jonathan S Cant, Mary-Ellen Large, Lindsay McCall, and Melvyn A Goodale. 2008. Independent processing of form, colour, and texture in object perception. *Perception* 37, 1 (2008), 57–78.

[15] Lai-Yu Cheng and Chiuhsiang Joe Lin. 2021. The effects of depth perception viewing on hand–eye coordination in virtual reality environments. *Journal of the Society for Information Display* 29, 10 (2021), 801–817.

[16] Yifei Cheng, Yukang Yan, Xin Yi, Yuanchun Shi, and David Lindlbauer. 2021. SemanticAdapt: Optimization-based Adaptation of Mixed Reality Layouts Leveraging Virtual-Physical Semantic Connections. In *UIST '21: The 34th Annual ACM Symposium on User Interface Software and Technology, Virtual Event, USA, October 10-14, 2021*, Jeffrey Nichols, Ranjitha Kumar, and Michael Nebeling (Eds.). ACM, 282–297. https://doi.org/10.1145/3472749.3474750

[17] James E Cutting. 1997. How the eye measures reality and virtual reality. *Behavior Research Methods, Instruments, & Computers* 29, 1 (1997), 27–36.

[18] Ciro Donalek, S. George Djorgovski, Alex Cioc, Anwell Wang, Jerry Zhang, Elizabeth Lawler, Stacy Yeh, Ashish Mahabal, Matthew J. Graham, Andrew J. Drake, Scott Davidoff, Jeffrey S. Norris, and Giuseppe Longo. 2014. Immersive and collaborative data visualization using virtual reality platforms. In *2014 IEEE International Conference on Big Data (IEEE BigData 2014), Washington, DC, USA, October 27-30, 2014*, Jimmy Lin, Jian Pei, Xiaohua Hu, Wo Chang, Raghunath Nambiar, Charu C. Aggarwal, Nick Cercone, Vasant G. Honavar, Jun Huan, Bamshad Mobasher, and Saumyadipta Pyne (Eds.). IEEE Computer Society, 609–614. https://doi.org/10.1109/BigData.2014.7004282

[19] Ruofei Du, Eric Turner, Maksym Dzitsiuk, Luca Prasso, Ivo Duarte, Jason Dourgarian, João Afonso, Jose Pascoal, Josh Gladstone, Nuno Cruces, Shahram Izadi, Adarsh Kowdle, Konstantine Tsotsos, and David Kim. 2020. DepthLab: Real-time 3D Interaction with Depth Maps for Mobile Augmented Reality. In *UIST '20: The 33rd Annual ACM Symposium on User Interface Software and Technology, Virtual Event, USA, October 20-23, 2020*, Shamsi T. Iqbal, Karon E. MacLean, Fanny Chevalier, and Stefanie Mueller (Eds.). ACM, 829–843. https://doi.org/10.1145/3379337.3415881

[20] Mark D Fairchild. 2013. *Color appearance models*. John Wiley & Sons.

[21] Ilja T Feldstein, Felix M Kölsch, and Robert Konrad. 2020. Egocentric distance perception: a comparative study investigating differences between real and virtual environments. *Perception* 49, 9 (2020), 940–967.

[22] Katherine Fennedy, Jeremy Hartmann, Quentin Roy, Simon Tangi Perrault, and Daniel Vogel. 2021. OctoPocus in VR: Using a Dynamic Guide for 3D Mid-Air Gestures in Virtual Reality. *IEEE Trans. Vis. Comput. Graph.* 27, 12 (2021), 4425–4438. https://doi.org/10.1109/TVCG.2021.3101854

[23] Devamardeep Hayatpur, Haijun Xia, and Daniel Wigdor. 2020. *DataHop: Spatial Data Exploration in Virtual Reality*. Association for Computing Machinery, New York, NY, USA, 818–828. https://doi.org/10.1145/3379337.3415878

[24] Teresa Hirzle, Fabian Fischbach, Julian Karlbauer, Pascal Jansen, Jan Gugenheimer, Enrico Rukzio, and Andreas Bulling. 2022. Understanding, Addressing, and Analysing Digital Eye Strain in Virtual Reality Head-Mounted Displays. *ACM Trans. Comput.-Hum. Interact.* 29, 4, Article 33 (mar 2022), 80 pages. https://doi.org/10.1145/3492802

[25] Nicolas S Holliman. 2004. Mapping perceived depth to regions of interest in stereoscopic images. In *Stereoscopic Displays and Virtual Reality Systems XI*, Vol. 5291. SPIE, 117–128.

[26] Ian P Howard. 2012. *Perceiving in depth, volume 1: basic mechanisms*. Oxford University Press.

[27] Peter Alan Howarth. 1999. Oculomotor changes within virtual environments. *Applied Ergonomics* 30, 1 (1999), 59–67.

[28] Fatima El Jamiy and Ronald Marsh. 2019. Survey on depth perception in head mounted displays: distance estimation in virtual reality, augmented reality, and mixed reality. *IET Image Process.* 13, 5 (2019), 707–712. https://doi.org/10.1049/iet-ipr.2018.5920

[29] Adam Jones, J. Edward Swan II, Gurjot Singh, Eric Kolstad, and Stephen R. Ellis. 2008. The effects of virtual reality, augmented reality, and motion parallax on egocentric depth perception. In *Proceedings of the 5th Symposium on Applied Perception in Graphics and Visualization, APGV 2008, Los Angeles, California, USA, August 9-10, 2008 (ACM International Conference Proceeding Series)*, Sarah H. Creem-Regehr and Karol Myszkowski (Eds.). ACM, 9–14. https://doi.org/10.1145/1394281.1394283

[30] Aiden Kang, Liang Wang, Ziyu Zhou, Zhe Huang, and Robert J. K. Jacob. 2021. Affective Color Fields: Reimagining Rothkoesque Artwork as an Interactive Companion for Artistic Self-Expression. In *MM '21: ACM Multimedia Conference, Virtual Event, China, October 20 - 24, 2021*, Heng Tao Shen, Yueting Zhuang, John R. Smith, Yang Yang, Pablo Cesar, Florian Metze, and Balakrishnan Prabhakaran (Eds.). ACM, 1454–1455. https://doi.org/10.1145/3474085.3478545

[31] Jonathan W. Kelly, Lucia A. Cherep, and Zachary D. Siegel. 2017. Perceived Space in the HTC Vive. *ACM Trans. Appl. Percept.* 15, 1 (2017), 2:1–2:16. https://doi.org/10.1145/3106155

[32] Eric Klein, J. Edward Swan II, Greg S. Schmidt, Mark A. Livingston, and Oliver G. Staadt. 2009. Measurement Protocols for Medium-Field Distance Perception in Large-Screen Immersive Displays. In *IEEE Virtual Reality Conference 2009 (VR 2009), 14-18 March 2009, Lafayette, Louisiana, USA, Proceedings*. IEEE Computer Society, 107–113. https://doi.org/10.1109/VR.2009.4811007

[33] Joshua M. Knapp and Jack M. Loomis. 2004. Limited Field of View of Head-Mounted Displays Is Not the Cause of Distance Underestimation in Virtual Environments. *Presence Teleoperators Virtual Environ.* 13, 5 (2004), 572–577. https://doi.org/10.1162/1054746042545238

[34] Robert Konrad, Anastasios Angelopoulos, and Gordon Wetzstein. 2020. Gaze-contingent ocular parallax rendering for virtual reality. *ACM Transactions on Graphics (TOG)* 39, 2 (2020), 1–12.

[35] Scott A. Kuhl, William B. Thompson, and Sarah H. Creem-Regehr. 2009. HMD calibration and its effects on distance judgments. *ACM Trans. Appl. Percept.* 6, 3 (2009), 19:1–19:20. https://doi.org/10.1145/1577755.1577762

[36] Marc Levoy and Pat Hanrahan. 1996. Light Field Rendering. In *Proceedings of the 23rd Annual Conference on Computer Graphics and Interactive Techniques, SIGGRAPH 1996, New Orleans, LA, USA, August 4-9, 1996*, John Fujii (Ed.). ACM, 31–42. https://doi.org/10.1145/237170.237199

[37] Adam Light and Patrick J Bartlein. 2004. The end of the rainbow? Color schemes for improved data graphics. *Eos, Transactions American Geophysical Union* 85, 40 (2004), 385–391.

[38] Chiuhsiang J Lin, Betsha T Abreham, and Bereket H Woldegiorgis. 2019. Effects of displays on a direct reaching task: A comparative study of head mounted display and stereoscopic widescreen display. *International Journal of Industrial Ergonomics* 72 (2019), 372–379.

[39] Yang Liu and Jeffrey Heer. 2018. Somewhere Over the Rainbow: An Empirical Assessment of Quantitative Colormaps. In *Proceedings of the 2018 CHI Conference on Human Factors in Computing Systems, CHI 2018, Montreal, QC, Canada, April 21-26, 2018*, Regan L. Mandryk, Mark Hancock, Mark Perry, and Anna L. Cox (Eds.). ACM, 598. https://doi.org/10.1145/3173574.3174172

[40] Diana Löffler, Robert Tscharn, and Jörn Hurtienne. 2018. Multimodal Effects of Color and Haptics on Intuitive Interaction with Tangible User Interfaces. In *Proceedings of the Twelfth International Conference on Tangible, Embedded, and Embodied Interaction, TEI 2018, Stockholm, Sweden, March 18-21, 2018*, Ylva Fernaeus, Donald McMillan, Martin Jonsson, Audrey Girouard, and Jakob Tholander (Eds.). ACM, 647–655. https://doi.org/10.1145/3173225.3173257

[41] JM Loomis, JW Philbeck, RL Klatzky, M Behrmann, and B MacWhinney. 2008. Measuring perception with spatial updating and action. Embodiment, ego-space, and action.

[42] Jack M Loomis, Joshua M Knapp, et al. 2003. Visual perception of egocentric distance in real and virtual environments. *Virtual and adaptive environments* 11 (2003), 21–46.

[43] Kenichiro Masaoka, Atsuo Hanazato, Masaki Emoto, Hirokazu Yamanoue, Yuji Nojiri, and Fumio Okano. 2006. Spatial distortion prediction system for stereoscopic images. *J. Electronic Imaging* 15, 1 (2006), 013002. https://doi.org/10.1117/1.2181178

[44] Sina Masnadi, Kevin P. Pfeil, Jose-Valentin T. Sera-Josef, and Joseph J. LaViola. 2021. Field of View Effect on Distance Perception in Virtual Reality. In *IEEE Conference on Virtual Reality and 3D User Interfaces Abstracts and Workshops, VR Workshops 2021, Lisbon, Portugal, March 27 - April 1, 2021*. IEEE, 542–543. https://doi.org/10.1109/VRW52623.2021.00153

[45] George Mather. 1996. Image blur as a pictorial depth cue. *Proceedings of the Royal Society of London. Series B: Biological Sciences* 263, 1367 (1996), 169–172.

[46] George Mather and David RR Smith. 2002. Blur discrimination and its relation to blur-mediated depth perception. *Perception* 31, 10 (2002), 1211–1219.

[47] Margaret W Matlin and Hugh J Foley. 1992. *Sensation and perception*. Allyn & Bacon.

[48] Michael Mauderer, Simone Conte, Miguel A. Nacenta, and Dhanraj Vishwanath. 2014. Depth perception with gaze-contingent depth of field. In *CHI Conference on Human Factors in Computing Systems, CHI'14, Toronto, ON, Canada - April 26 - May 01, 2014*, Matt Jones, Philippe A. Palanque, Albrecht Schmidt, and Tovi

Grossman (Eds.). ACM, 217–226. https://doi.org/10.1145/2556288.2557089
[49] Michael Mauderer, David R. Flatla, and Miguel A. Nacenta. 2016. Gaze-Contingent Manipulation of Color Perception. In *Proceedings of the 2016 CHI Conference on Human Factors in Computing Systems, San Jose, CA, USA, May 7-12, 2016*, Jofish Kaye, Allison Druin, Cliff Lampe, Dan Morris, and Juan Pablo Hourcade (Eds.). ACM, 5191–5202. https://doi.org/10.1145/2858036.2858320
[50] Ravi Mehta and Rui Zhu. 2009. Blue or red? Exploring the effect of color on cognitive task performances. *Science* 323, 5918 (2009), 1226–1229.
[51] Mark Mon-Williams and James R Tresilian. 2000. Ordinal depth information from accommodation? *Ergonomics* 43, 3 (2000), 391–404.
[52] Kenneth Moreland. 2009. Diverging Color Maps for Scientific Visualization. In *Advances in Visual Computing, 5th International Symposium, ISVC 2009, Las Vegas, NV, USA, November 30 - December 2, 2009, Proceedings, Part II (Lecture Notes in Computer Science, Vol. 5876)*, George Bebis, Richard D. Boyle, Bahram Parvin, Darko Koracin, Yoshinori Kuno, Junxian Wang, Renato Pajarola, Peter Lindstrom, André Hinkenjann, L. Miguel Encarnação, Cláudio T. Silva, and Daniel S. Coming (Eds.). Springer, 92–103. https://doi.org/10.1007/978-3-642-10520-3_9
[53] Alessio Murgia and Paul M. Sharkey. 2009. Estimation of Distances in Virtual Environments Using Size Constancy. *Int. J. Virtual Real.* 8, 1 (2009), 67–74. https://doi.org/10.20870/IJVR.2009.8.1.2714
[54] Michael Nebeling, Maximilian Speicher, Xizi Wang, Shwetha Rajaram, Brian D. Hall, Zijian Xie, Alexander R. E. Raistrick, Michelle Aebersold, Edward G. Happ, Jiayin Wang, Yanan Sun, Lotus Zhang, Leah E. Ramsier, and Rhea Kulkarni. 2020. *MRAT: The Mixed Reality Analytics Toolkit.* Association for Computing Machinery, New York, NY, USA, 1–12. https://doi.org/10.1145/3313831.3376330
[55] Cuong Nguyen, Stephen DiVerdi, Aaron Hertzmann, and Feng Liu. 2018. Depth Conflict Reduction for Stereo VR Video Interfaces. In *Proceedings of the 2018 CHI Conference on Human Factors in Computing Systems, CHI 2018, Montreal, QC, Canada, April 21-26, 2018*, Regan L. Mandryk, Mark Hancock, Mark Perry, and Anna L. Cox (Eds.). ACM, 64. https://doi.org/10.1145/3173574.3173638
[56] Ekaterina Olshannikova, Aleksandr Ometov, Yevgeni Koucheryavy, and Thomas Olsson. 2015. Visualizing Big Data with augmented and virtual reality: challenges and research agenda. *J. Big Data* 2 (2015), 22. https://doi.org/10.1186/s40537-015-0031-2
[57] Robert P O'Shea, Donovan G Govan, and Robert Sekuler. 1997. Blur and contrast as pictorial depth cues. *Perception* 26, 5 (1997), 599–612.
[58] Kevin Pfeil, Sina Masnadi, Jacob Belga, Jose-Valentin T. Sera-Josef, and Joseph J. LaViola. 2021. Distance Perception with a Video See-Through Head-Mounted Display. In *CHI '21: CHI Conference on Human Factors in Computing Systems, Virtual Event / Yokohama, Japan, May 8-13, 2021*, Yoshifumi Kitamura, Aaron Quigley, Katherine Isbister, Takeo Igarashi, Pernille Bjørn, and Steven Mark Drucker (Eds.). ACM, 528:1–528:9. https://doi.org/10.1145/3411764.3445223
[59] Jiamin Ping, Bruce H Thomas, James Baumeister, Jie Guo, Dongdong Weng, and Yue Liu. 2020. Effects of shading model and opacity on depth perception in optical see-through augmented reality. *Journal of the Society for Information Display* 28, 11 (2020), 892–904.
[60] Matthieu Poyade, Arcadio Reyes-Lecuona, and Raquel Viciana-Abad. 2009. Influence of binocular disparity in depth perception mechanisms in virtual environments. In *New Trends on Human–Computer Interaction*. Springer, 13–22.
[61] K Prazdny. 1980. Egomotion and relative depth map from optical flow. *Biological cybernetics* 36, 2 (1980), 87–102.
[62] Dennis R Proffitt and Corrado Caudek. 2013. Depth perception and the perception of events. (2013).
[63] Penny L Rheingans. 2000. Task-based color scale design. In *28th AIPR Workshop: 3D Visualization for Data Exploration and Decision Making*, Vol. 3905. SPIE, 35–43.
[64] Bernice E Rogowitz and Lloyd A Treinish. 1998. Data visualization: the end of the rainbow. *IEEE spectrum* 35, 12 (1998), 52–59.
[65] Christoph Rößing, Johannes Hanika, and Hendrik P. A. Lensch. 2012. Real-Time Disparity Map-Based Pictorial Depth Cue Enhancement. *Comput. Graph. Forum* 31, 2pt1 (2012), 275–284. https://doi.org/10.1111/j.1467-8659.2012.03006.x
[66] Cynthia S. Sahm, Sarah H. Creem-Regehr, William B. Thompson, and Peter Willemsen. 2005. Throwing versus walking as indicators of distance perception in similar real and virtual environments. *ACM Trans. Appl. Percept.* 2, 1 (2005), 35–45. https://doi.org/10.1145/1048687.1048690
[67] Pavel Senin. 2008. Dynamic time warping algorithm review. *Information and Computer Science Department University of Hawaii at Manoa Honolulu, USA* 855, 1-23 (2008), 40.
[68] Samuel S. Silva, Beatriz Sousa Santos, and Joaquim Madeira. 2011. Using color in visualization: A survey. *Comput. Graph.* 35, 2 (2011), 320–333. https://doi.org/10.1016/j.cag.2010.11.015
[69] Stephen Smart and Danielle Albers Szafir. 2019. Measuring the Separability of Shape, Size, and Color in Scatterplots. In *Proceedings of the 2019 CHI Conference on Human Factors in Computing Systems, CHI 2019, Glasgow, Scotland, UK, May 04-09, 2019*, Stephen A. Brewster, Geraldine Fitzpatrick, Anna L. Cox, and Vassilis Kostakos (Eds.). ACM, 669. https://doi.org/10.1145/3290605.3300899
[70] Geb Thomas, Joseph H. Goldberg, David J. Cannon, and Steven L. Hillis. 2002. Surface Textures Improve the Robustness of Stereoscopic Depth Cues. *Hum. Factors* 44, 1 (2002), 157–170. https://doi.org/10.1518/0018720024494766
[71] William B. Thompson, Peter Willemsen, Amy Ashurst Gooch, Sarah H. Creem-Regehr, Jack M. Loomis, and Andrew C. Beall. 2004. Does the Quality of the Computer Graphics Matter when Judging Distances in Visually Immersive Environments? *Presence Teleoperators Virtual Environ.* 13, 5 (2004), 560–571. https://doi.org/10.1162/1054746042545292
[72] Tom Troscianko, Rachel Montagnon, Jacques Le Clerc, Emmanuelle Malbert, and Pierre-Louis Chanteau. 1991. The role of colour as a monocular depth cue. *Vision research* 31, 11 (1991), 1923–1929.
[73] Cyril Vienne, Stéphane Masfrand, Christophe Bourdin, and Jean-Louis Vercher. 2020. Depth Perception in Virtual Reality Systems: Effect of Screen Distance, Environment Richness and Display Factors. *IEEE Access* 8 (2020), 29099–29110. https://doi.org/10.1109/ACCESS.2020.2972122
[74] Margarita Vinnikov and Robert S. Allison. 2014. Gaze-contingent depth of field in realistic scenes: the user experience. In *Eye Tracking Research and Applications, ETRA '14, Safety Harbor, FL, USA, March 26-28, 2014*, Pernilla Qvarfordt and Dan Witzner Hansen (Eds.). ACM, 119–126. https://doi.org/10.1145/2578153.2578170
[75] Colin Ware. 1988. Color sequences for univariate maps: theory, experiments and principles. *IEEE Computer Graphics and Applications* 8, 5 (1988), 41–49. https://doi.org/10.1109/38.7760
[76] Zachary Wartell, Larry F. Hodges, and William Ribarsky. 1999. Balancing Fusion, Image Depth and Distortion in Stereoscopic Head-Tracked Displays. In *Proceedings of the 26th Annual Conference on Computer Graphics and Interactive Techniques, SIGGRAPH 1999, Los Angeles, CA, USA, August 8-13, 1999*, Warren N. Waggenspack (Ed.). ACM, 351–358. https://doi.org/10.1145/311535.311587
[77] Daniel Weiskopf and Thomas Ertl. 2002. A depth-cueing scheme based on linear transformations in tristimulus space. (2002).
[78] Wikipedia contributors. 2021. Distance fog — Wikipedia, The Free Encyclopedia. https://en.wikipedia.org/w/index.php?title=Distance_fog&oldid=1061783656 [Online; accessed 27-March-2022].
[79] Wikipedia contributors. 2021. Range imaging — Wikipedia, The Free Encyclopedia. https://en.wikipedia.org/wiki/Depth_map [Online; accessed 27-March-2022].
[80] Peter Willemsen, Mark B. Colton, Sarah H. Creem-Regehr, and William B. Thompson. 2004. The effects of head-mounted display mechanics on distance judgments in virtual environments. In *Proceedings of the 1st Symposium on Applied Perception in Graphics and Visualization, APGV 2004, Los Angeles, California, USA, August 7-8, 2004 (ACM International Conference Proceeding Series, Vol. 73)*, Victoria Interrante, Ann McNamara, Heinrich H. Bülthoff, and Holly E. Rushmeier (Eds.). ACM, 35–38. https://doi.org/10.1145/1012551.1012558
[81] Peter Willemsen, Amy Ashurst Gooch, William B. Thompson, and Sarah H. Creem-Regehr. 2008. Effects of Stereo Viewing Conditions on Distance Perception in Virtual Environments. *Presence Teleoperators Virtual Environ.* 17, 1 (2008), 91–101. https://doi.org/10.1162/pres.17.1.91
[82] Bob G. Witmer and Wallace J. Sadowski. 1998. Nonvisually Guided Locomotion to a Previously Viewed Target in Real and Virtual Environments. *Hum. Factors* 40, 3 (1998), 478–488. https://doi.org/10.1518/001872098779591340
[83] Emilie Yu, Rahul Arora, Tibor Stanko, Jakob Andreas Bærentzen, Karan Singh, and Adrien Bousseau. 2021. CASSIE: Curve and Surface Sketching in Immersive Environments. In *CHI '21: CHI Conference on Human Factors in Computing Systems, Virtual Event / Yokohama, Japan, May 8-13, 2021*, Yoshifumi Kitamura, Aaron Quigley, Katherine Isbister, Takeo Igarashi, Pernille Bjørn, and Steven Mark Drucker (Eds.). ACM, 190:1–190:14. https://doi.org/10.1145/3411764.3445158
[84] Xue Yu, Stephen DiVerdi, Akshay Sharma, and Yotam I. Gingold. 2021. ScaffoldSketch: Accurate Industrial Design Drawing in VR. In *UIST '21: The 34th Annual ACM Symposium on User Interface Software and Technology, Virtual Event, USA, October 10-14, 2021*, Jeffrey Nichols, Ranjitha Kumar, and Michael Nebeling (Eds.). ACM, 372–384. https://doi.org/10.1145/3472749.3474756
[85] Yuhang Zhao, Edward Cutrell, Christian Holz, Meredith Ringel Morris, Eyal Ofek, and Andrew D. Wilson. 2019. SeeingVR: A Set of Tools to Make Virtual Reality More Accessible to People with Low Vision. In *Proceedings of the 2019 CHI Conference on Human Factors in Computing Systems, CHI 2019, Glasgow, Scotland, UK, May 04-09, 2019*, Stephen A. Brewster, Geraldine Fitzpatrick, Anna L. Cox, and Vassilis Kostakos (Eds.). ACM, 111. https://doi.org/10.1145/3290605.3300341
[86] Liang Zhou and Charles D. Hansen. 2016. A Survey of Colormaps in Visualization. *IEEE Trans. Vis. Comput. Graph.* 22, 8 (2016), 2051–2069. https://doi.org/10.1109/TVCG.2015.2489649